View metadata, citation and similar papers at core.ac.uk

brought to you by CORE

provided by e_Buah - Biblioteca Digital de la Universidad de Alcalá

Universidad de Alcalá

BIBLIOTECA

Document downloaded from the institutional repository of the University of Alcala: http://ebuah.uah.es/dspace/

This is a preprint version of the following published document:

Regadío, A., Tabero, J. & Sánchez-Prieto, S. 2016, "Impact of colored noise in pulse amplitude measurements: a time-domain approach using differintegrals", Nuclear Instruments and Methods in Physics Research Section A, vol. 811, pp. 25-29

Available at https://doi.org/10.1016/j.nima.2015.12.010

© 2016 Elsevier

(Article begins on next page)

This work is licensed under a

Creative Commons Attribution-NonCommercial-NoDerivatives 4.0 International License.

Impact of colored noise in pulse amplitude measurements: a time-domain approach using differintegrals

Alberto Regadío[a,b,*], Jesús Tabero[a], Sebastián Sánchez-Prieto[b]

[a] *Electronic Technology Area, Instituto Nacional de Técnica Aeroespacial, 28850 Torrejón de Ardoz, Spain*
[b] *Department of Computer Engineering, Space Research Group, Universidad de Alcalá, 28805 Alcalá de Henares, Spain*

Abstract

In particle detectors, pulse shaping is the process of changing the waveform of the pulses in order to maximize the signal to noise ratio. This shaping usually only takes into account white, pink (flicker) and red (brownian) noise. In this paper, a generalization of noise indexes as a function to an arbitrary f^β noise type, where β is a real number, is presented. This generalization has been created using the differintegral operator, defined in Fractional Calculus. These formulas are used to calculate the Equivalent Noise Change (ENC) in detector particle systems.

Keywords: Spectroscopy, Noise, Shaping, Digital Signal Processing, Resolution

1. Introduction

In spectroscopy systems, pulse shaping plays a crucial role in noise filtering. In order to analyze different shaping modes, Goulding [1] and Radeka [2] defined the noise indexes of shapers (also called “form factors” in [3]) as parameters proportional to the contribution of a specific noise type. These parameters only depend on the pulse shape and its duration. A different noise index has to be calculated for each different “color of noise”. In a signal with components at all frequencies and a power spectral density per unit of bandwidth proportional to f^β, the color is given by the β value. For instance, the spectral density of white noise is flat ($\beta = 0$), while pink (flicker) noise has $\beta = -1$ and red (brownian) noise has $\beta = -2$.

In this paper, all the noise spectral densities are referred to the preamplifier output. Goulding [1] calculated the noise indexes for voltage (white) and current (red) noise at this point of the circuit. In [4] the f^{-1} (pink) noise index using the concept of 1/2-derivative developed in Fractional Calculus [5] was also introduced. A strength of noise indexes is that they are calculated in time-domain directly whereas other methods that use Fourier Transforms are less intuitive and more complex to carry out. The first conclusion taken from the noise indexes is that the contribution from red noise increases with shaping time whereas

*Corresponding Author

Email addresses: regadioca@inta.es (Alberto Regadío), taberogj@inta.es (Jesús Tabero), sebastian.sanchez@uah.es (Sebastián Sánchez-Prieto)

the white noise contribution decreases. The f^{-1} noise does not depend on the shaping time. Fig. 1 shows a typical example of ENC at shaper output vs. shaping time in presence of red and white noise.

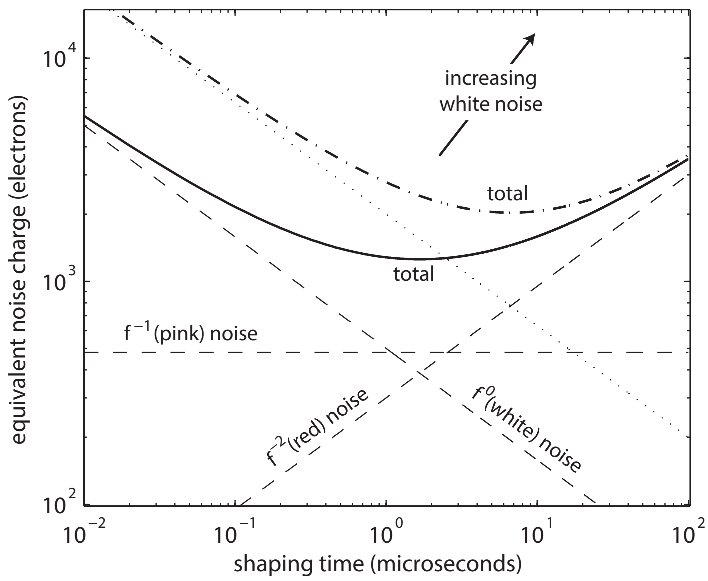

Figure 1: Equivalent noise charge vs. shaping time. Changing the red noise ($\beta = -2$) or, as in this case, white noise ($\beta = 0$) contribution shifts the noise minimum. Increased voltage noise is shown as an example. (Figure reproduced from [3]) with permission.

Until now, noise analysis have been performed just for white, pink and red noise (e.g. [6]), which are proportional to f^{-2}, f^{-1} and f^{0} respectively. However, in particle detectors, noise distribution is often more complex. In fact, the most common noise in particle detectors has a continuous range from $f^{-0.5}$ to f^{-2} [7, 8]. In this paper, a generalization of the noise indexes using differintegrals is proposed with the aim of covering a continuous desired range, instead of using only discrete values such as f^{-2}, f^{-1} or f^{0}. With this generalization, shapers can be analyzed more deeply.

In principle, this analysis can be used to obtain the generalized noise parameters of a shaper. This analysis can be used individually, or as a cost function of an automated algorithm to find the optimal shaping. Moreover, this method also allows analyzing a shaper, provided by optimization algorithms, to find the predominant noise type present in the system, and then try to mitigate it. There is extensive material published on optimal pulse shaping synthesis (e.g. [9–12]).

Finally, we would like to clarify that this paper focuses on noise impact measurement, but does not focus on selecting the most suitable pulse shape for a given spectroscopy system or particle detector; instead, in this paper we describe a method to analyze the relative noise performance of pulse-shaping systems.

2. Differintegrals

Whenever a function $W(t)$ is derived n (positive integer) times or integrated $-n$ times, we can replace n for a real number α. If $\alpha > 0$, $W^{(\alpha)}(t)$ is the α fractional derivative of $W(t)$. Otherwise, $W^{(\alpha)}(t)$ is the $-\alpha^{th}$ fractional integral. Differintegrals are a combined fractional differentiation/integration operator. Therefore, $W^{(\alpha)}(t)$ is the Differintegral operator [5] applied to $W(t)$. Actually, α can be also a imaginary number [13] leading to complex-order derivatives. However, for our purposes, it is sufficient that α be a real number.

In literature, there are several definitions of fractional derivative and integral [14]. Thus, to define the differintegral operator, it must be defined first fractional derivatives and integrals separately.

On one hand, the classical form of fractional integral is the Riemann–Liouville definition:

$$J^{\alpha} f(t) := \frac{1}{\Gamma(\alpha)} \int_0^t (t-\tau)^{\alpha-1} f(\tau)\, d\tau \tag{1}$$

where α is a real positive number, Γ is the Gamma Function and J is the Riemann–Liouville integral operator.

On the other hand, the definition of Riemann–Liouville fractional derivative is based in the previous formula and is given by:

$$D^{\alpha} f(t) := \frac{1}{\Gamma(n-\alpha)} \frac{d^n}{dt^n} \left(\int_0^t (t-\tau)^{n-\alpha-1} f(\tau)\, d\tau \right) \tag{2}$$

where n is an integer number. This equation is the cornerstone of fractional calculus.

Although both operators are linear, J commutes (i.e. $J^{\alpha} J^{\beta} f(t) = J^{\beta} J^{\alpha} f(t)$). However, D does not commute for non-integer numbers, that is $J^{\alpha} D^{\alpha} f(t) \neq D^{\alpha} J^{\alpha} f(t)$. In addition $D^{\alpha} k$ for any constant k is not always equal to 0. To solve these drawbacks, alternative definitions for fractional derivatives were proposed. One of the most popular is the Caputo derivative, also based in Eq. (1):

$$D_c^{\alpha} f(t) := J^{\lceil \alpha \rceil - \alpha} D^{\lceil \alpha \rceil} f(t) \tag{3}$$

where $\lceil \alpha \rceil$ is the ceiling function, which provides the smallest integer greater than or equal to α. Then, in this case, the value of $D^{\lceil \alpha \rceil} f(t)$ is a derivative of integer value. This new operator is linear and commutes, that is $J^{\alpha} D_c^{\alpha} f(t) = D_c^{\alpha} J^{\alpha} f(t)$, and $D_c^{\alpha} k = 0$ for any constant k. Both operators, J and D_c form the differintegral operator. However, both J and D_c are complex to calculate by means of numerical methods.

To approximate the value of the differintegral, instead of J and D_c operators, in this paper and henceforth we are going to use the Grünwald–Letnikov definition given by:

$$f^{(\alpha)}(t) = \lim_{h \to 0} \frac{1}{h^{\alpha}} \sum_{j=0}^{k} (-1)^j \binom{\alpha}{j} f(kh - jh) \tag{4}$$

This formula is easily implemented using numerical methods [16] compared to (1) and (3) and it has been used in another works related to filters and numerical calculus (e.g. [17]).

3. Generalization of the ENC Formula

As a starting point, we are going to use the ENC formula presented in [3, 8] because it is necessary to know the noise indexes to be calculated. The ENC formula is:

$$Q_n^2 = i_n^2 F_i \tau_s + v_n^2 F_v \frac{C^2}{\tau_s} + F_{vf} A_f C^2 \tag{5}$$

where Q_n is the ENC in Coulombs, τ_s is the total shaping time and C is the equivalent detector capacitance. F_v, F_i, and F_{vf} are the noise indexes for f^0-noise, f^{-2}-noise and f^{-1}-noise, respectively; in this nomenclature, they are dimensionless. i_n is the current noise spectral density measured in $\mathrm{A}/\sqrt{\mathrm{Hz}}$, v_n is the voltage noise spectral density measured in $\mathrm{V}/\sqrt{\mathrm{Hz}}$, A_f is the f^{-1}-noise spectral density coefficient measured in V^2. The f^{-1}-noise spectral density v_{nf} is equal to:

$$v_{nf} = \sqrt{\frac{A_f}{f}} \;\; [\mathrm{V}/\sqrt{\mathrm{Hz}}] \tag{6}$$

Others nomenclatures different than the one proposed in [3] such as [8, 15] are equivalent. The Eq. (5) is applicable to both analog and digital shapers.

The value of F_i and F_v are:

$$F_i = \frac{1}{2\tau_s} \int_{-\infty}^{\infty} W^2(t)\, dt \tag{7}$$

$$F_v = \frac{\tau_s}{2} \int_{-\infty}^{\infty} \left(W'(t)\right)^2 dt \tag{8}$$

where for time-invariant pulse shaping $W(t)$ is the system's impulse response for a short input pulse with the peak output signal normalized to unity. For time-variant systems (e.g. gated integrators), $W(t)$ can be also easily calculated according to the method described in [1]. An alternative notation of these last two formulas can be found in the same reference.

The expression for F_{vf} can be deduced from [4, 15] and is equal to:

$$F_{vf} = \frac{1}{2} \int_{-\infty}^{\infty} \left(W^{(1/2)}(t)\right)^2 dt \tag{9}$$

where $W^{(1/2)}(t)$ is the 1/2-derivative of $W(t)$. It must be taken into account that the calculus of the 1/2-derivative in time domain is equivalent to multiply by $\sqrt{s}$ in Laplace domain. There are several methods (analytical and numerical) to calculate the fractional derivatives [5]. One of the simplest for 1/2-derivative calculation was proposed in [4]:

$$W^{(1/2)}(t) = \frac{1}{\sqrt{\pi t}} * W'(t), \forall t > 0 \tag{10}$$

These three formulas could be generalized in a continuous noise index:

$$F(\beta) = \frac{1}{2}\tau_s^{\beta+1}\int_{-\infty}^{\infty}\left(W^{(1+\frac{\beta}{2})}(t)\right)^2 dt \tag{11}$$

Note that $F(0) = F_v$, $F(-1) = F_{vf}$ and $F(-2) = F_i$. Thus, in line with the formulas of [15], the following generalization of (5) is proposed:

$$Q_n^2 = \int_{-\infty}^{\infty} C^2 v_n^2(\beta) F(\beta) \tau_s^{-\beta-1}\, d\beta \tag{12}$$

where $v_n^2(\beta)$ is the converted voltage noise spectral density. Specific values for this parameter are:

$$v_n^2(0) = v_n^2 \ [\mathrm{V}^2/\mathrm{Hz}]$$

$$v_n^2(-1) = A_f \ [\mathrm{V}^2]$$

$$v_n^2(-2) = A_i \equiv (i_n/C)^2 \ [\mathrm{V}^2 \cdot \mathrm{Hz}]$$

This last formula is also applicable when we want to to translate current noise spectral densities to voltage.

If only specific types of noise (i.e. β values) are considered, Eq. (12) can be simplified as follows:

$$Q_n^2 = \sum_i C^2 v_{n_i}^2(\beta) F_i(\beta) \tau_s^{-\beta-1} \tag{13}$$

where i indicates the noise type considered.

Notice that, according to Eq. (11) for all the values of β, except $\beta = -1$, the value of $F(\beta)$ depends on τ_s. Thus, when τ_s is changed, the total noise can go through a minimum, where the main noise contributions are equal. Thus, the contribution from noise whose $\beta < -1$ increases with shaping time whereas the noise whose $\beta > -1$ decreases with increasing shaping time. f^{-1} noise does not depends on the shaping because $\beta = -1$. This allows to adjust the shaping time to shift the noise minimum as shown in example of Fig. 2.

It can be seen in both Fig. 1 and Fig. 2, that noises with $\beta > -1$ dominate at short shaping times, whereas at long shaping times, $\beta < -1$ noises takes over. This fact is shown in Fig. 3 where Q_n vs. shaping time for several β noise contribution is presented. In Fig. 3 $\beta = -2$ and $\beta = 0$, corresponding to red and white noise respectively, are highlighted.

4. Noise curves of CR–(RC)^n shapers

To test the behavior of Eq. (11), the value of $F(\beta)$ has been calculated for one of the most common analog shapers: CR–(RC)^n. The differintegrals for $F(\beta)$ was obtained using the function *gdiff* presented in [16] that implements the Grünwald–Letnikov Method, presented in Section 2.

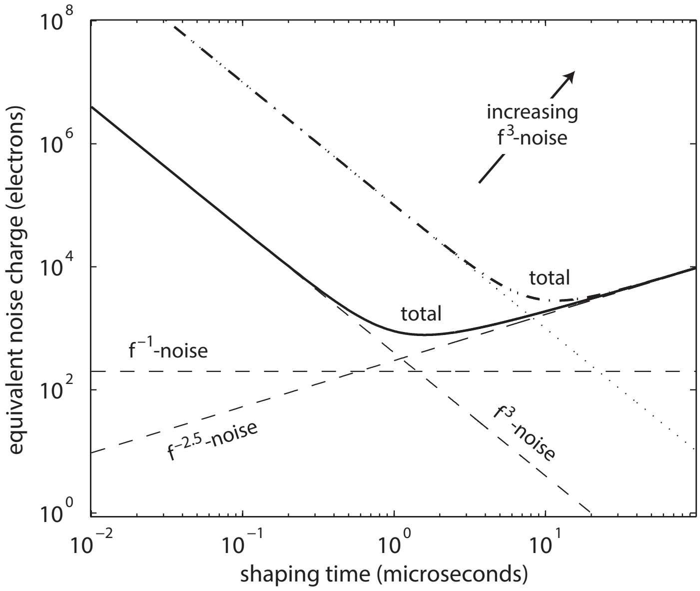

Figure 2: Equivalent noise charge vs. shaping time for arbitrary β noise contribution. In this case $\beta = 3$ and $\beta = -2.5$. As in Fig. 1 changing the noise contribution shifts the noise minimum.

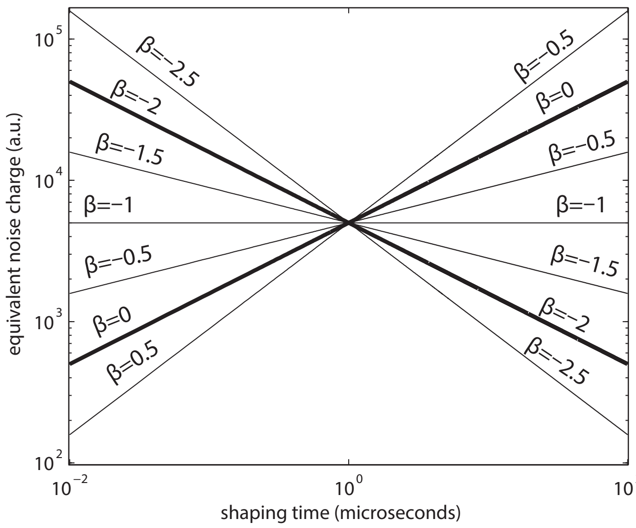

Figure 3: Equivalent noise charge vs. shaping time for several β noise contribution.

Fig. 4 depicts $F(\beta)$ for CR shaping. This type of shaping generates the following decreasing exponential function when a particle is detected:

$$x(t) = A \, \exp\left(\frac{-t}{\tau_1}\right) \tag{14}$$

where A is the pulse height and $\tau_1 = CR$ is the decay constant. The anomalously high value of τ_1 has been chosen to show the figure as clearly as possible. Otherwise the $F(\beta)$ values for red noise would be negligible with respect to blue or vice versa.

We can see that for $\beta < 2$ the value of $F(\beta)$ is dramatically increased due to the pulse duration that implies a high τ_1. Also, for a noise spectrum of $\beta \approx -0.3$ the effect of increasing τ_1 has almost no effect on $F(\beta)$.

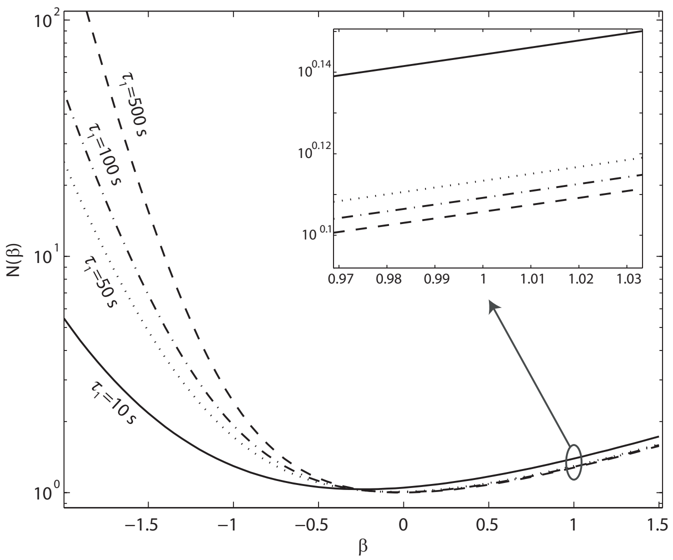

Figure 4: Continuous noise index of the shapers for CR shaping for several τ_1.

Fig. 5 shows the value of $F(\beta)$, in this case, for CR–RC shaping. This type of shaping generates the following pulse when a particle is detected:

$$x(t) = A\,\frac{-t}{\tau_1 - \tau_2}\left(\exp\left(\frac{-t}{\tau_1}\right) - \exp\left(\frac{-t}{\tau_2}\right)\right) \tag{15}$$

where $\tau_2 = RC$ is the decay constant at the second state of the shaper. The height of each shaper was normalized, so that every $x(t)$ has the same height.

Fig. 6 depicts the value of $F(\beta)$ for the CR–(RC)^n (n from 0 to 5) shapers. For simplicity, the same τ was set in all the stages of each shaper. Thus, the following pulse is generated:

$$x(t) = \frac{A}{n!}\left(\frac{t}{\tau}\right)^n \exp\left(\frac{-t}{\tau}\right) \tag{16}$$

The height of each shaper has also been normalized, so that every shaper has the same height. Obviously, the duration of each pulse is variable depending on n. Again, this high value was chosen to show the figure as clearly as possible.

According to Section 3, when the value of τ decreases, $F(\beta > -1)$ increases while $F(\beta < -1)$ decreases, as if a rotation around the $F(\beta = -1)$ axis is involved. For $\beta < -2$, all values of $N(\beta)$ are ∞ in the three

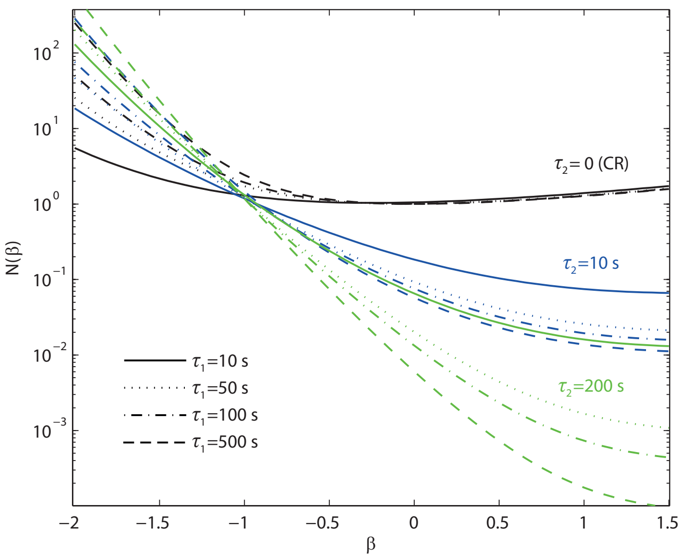

Figure 5: Continuous noise index of the previous CR shapers and CR–RC shapers.

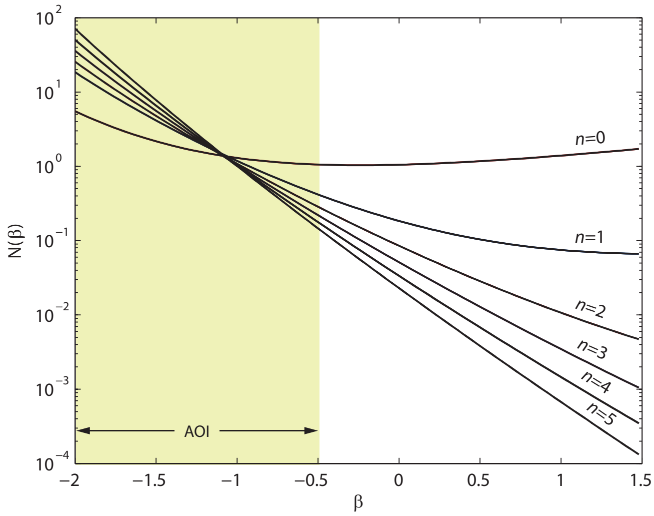

Figure 6: Continuous noise index of CR–(RC)^n shapers. It is also marked the Area Of Interest (AOI) $-2 < \beta < -0.5$ designated by [7].

figures. As it can be noted in Fig. 6, the effect of increasing τ_1 or τ_2 for noises of $\beta \approx -1$ does not have any effect on $F(\beta)$.

5. Noise curves of the most common optimal digital shapers

In Fig. 7 the normalized impulse response of some of the most common optimal digital shapers: (1) optimal for white noise; (2) optimal for f^{-1}-noise [19]; (3) optimal for f^{-2}-noise; (4) optimal for f^{-3}-noise ($1/f$ current noise) [9] are presented.

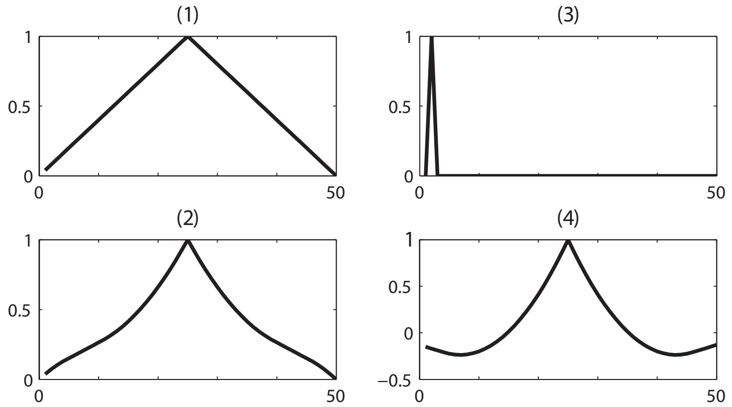

Figure 7: Normalized response of some of the most common optimal digital shapers: optimal for (1) white noise, (2) f^{-1} noise, (3) f^{-2} noise, (4) f^{-3} noise.

The value of $F(\beta)$ for these shapers is shown in Fig. 8. The differintegrals for $F(\beta)$ were also obtained using the function *gdiff*. In this figure, $F(\beta)$ was calculated for a τ_s =5 s (0.1 s/sample). As in previous section, this anomalously high value of τ_s was chosen so that the values of $F(\beta)$ were more legible. For a given value of τ_s, Shaper 1 has the minimum F for $\beta = 0$, Shaper 2 has the minimum F for $\beta = -1$, Shaper 3 has the minimum F for $\beta = -2$ and Shaper 4 has the minimum F for $\beta = -3$. These values, marked with a black square (■) are optimal for each noise type.

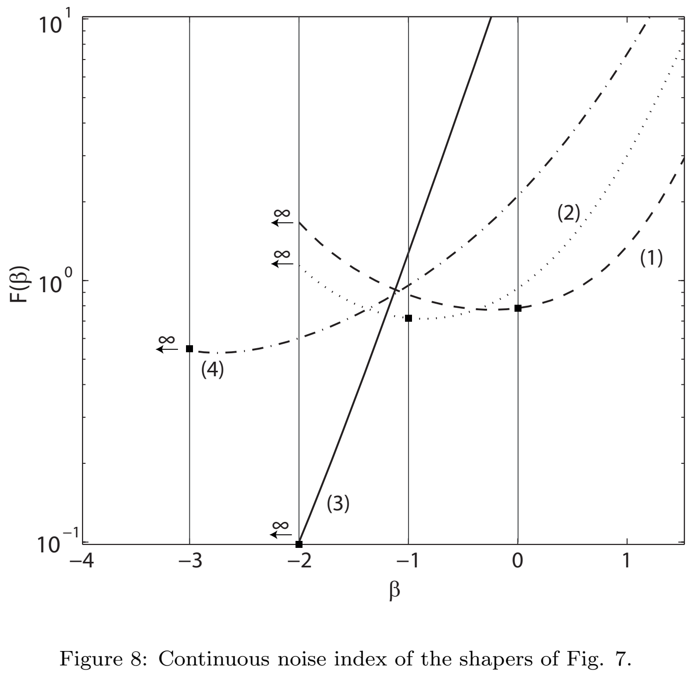

Figure 8: Continuous noise index of the shapers of Fig. 7.

In Fig. 8 the $F(\beta)$ values for $\beta < -2$ are not drawn because they tend to ∞ for all shapers except for 4. This is because the shaper 4 output provides values below zero that allow the 1/2-integral ($\beta = -3$ in Eq.

(11)) return to 0. This is required so that $F(\beta) < \infty$. In the same way, for bipolar shapers with equal area above and below zero, $F(-4) < \infty$ because the integral of (11) returns to 0. Such observations are not as easy to perform when working in the frequency domain. It is also important to take into account that most detectors nowadays have negligible values for f^{β}-noise, $\beta < -2$.

6. Conclusion

A generalization of noise indexes in function to an arbitrary f^{β} noise, where β is a real number, has been presented. Thus, with this new continuous noise index, shapers can be analyzed more deeply allowing to choose a better shaping system for a given particle detector. The simplicity of resolution calculations using the presented method has been demonstrated here. These formulas may also be applied to measure the ENC (i.e. signal/noise ratio) in other disciplines which involved transients processing.

Acknowledgments

This project was funded by the Spanish Administration as part of projects ref. AYA2011-29727-C02-02 and AYA2012-39810-C02-02.

References

[1] F. S. Goulding, Nuclear Instruments and Methods 100 (1972) 493.
[2] V. Radeka, Ann. Rev. Nucl. Part. Sci. 1988 38:217.
[3] K. A. Olive et al. (Particle Data Group), Chinese Physics C38, 090001 (2014) 432.
[4] A. Pullia, Nuclear Instruments and Methods in Physics Research A 405 (1998) 121.
[5] R. Gorenflo, F. Mainardi, Fractional calculus. Springer Vienna, 1997.
[6] D. Avila, E. Álvarez, A. Abusleme, IEEE Transactions on Nuclear Science, vol. 60, no. 6, Dec. 2013.
[7] H. Spieler, Semiconductor Detector Systems, Oxford University Press, Oxford, 2005.
[8] H. Spieler, Nuclear Instruments and Methods in Physics Research A 636 (2011) S149.
[9] E. Gatti, A. Geraci, G. Ripamonti, Nuclear Instruments and Methods in Physics Research A 394 (1997) 268.
[10] W. Gao, B. Gan, X. Li, T. Wei, D. Gao, Y. Hu, Nuclear Instruments and Methods in Physics Research A 780 (2015) 15.
[11] A. Regadío, S. Sánchez-Prieto, J. Tabero, Nuclear Instruments and Methods in Physics Research A 738 (2014) 74.
[12] A. Regadío, S. Sánchez-Prieto, J. Tabero, Nuclear Instruments and Methods in Physics Research A 795 (2015) 115.
[13] E. R. Love, J. London Math. Soc. (2), 3 (1971), 241–259.
[14] E. Capelas, J. A. Tenreiro, Mathematical Problems in Engineering (2014) http://dx.doi.org/10.1155/2014/238459
[15] E. Gatti, A. Geraci, G. Ripamonti, Nuclear Instruments and Methods in Physics Research A 381 (1996) 117.
[16] C. Chunmei, G. Feng, Journal of Software vol. 8, no. 3 (2013) 572.
[17] C.-C. Tseng, S.-L. Lee, Signal Processing 92 (2012) 1317.
[18] K. Diethelm, N.J. Ford, A.D. Freed, Yu. Luchko, Comput. Methods Appl. Mech. Engrg. 194 (2005) 743.
[19] E. Gatti, M. Sampietro, P. F. Manfredi, Nuclear Instruments and Methods in Physics Research A 287 (1990) 513.